Highly Stable Optically Induced Birefringence and Holographic Surface Gratings on a New Azocarbazole-Based Polyimide

Jian Ping Chen,[†] François Lagugné Labarthet,[‡] Almeria Natansohn,*[,†] and Paul Rochon[‡]

Department of Chemistry, Queen's University, Kingston, Ontario, Canada K7L 3N6, and Department of Physics, Royal Military College, Kingston, Ontario, Canada K7K 5L0

Received May 14, 1999; Revised Manuscript Received August 23, 1999

ABSTRACT: An azocarbazole-based polyimide was synthesized from an azocarbazole diamine monomer and 4,4′-(hexafluoroisopropylidene)diphthalic anhydride (6FDA) by a two-step polycondensation reaction. Birefringence experiments have been performed on the pure polyimide and on the polyimide mixed with small azo chromophores. Because of its high T_g, the polyimide has a very stable induced birefringence (only 14% loss during the relaxation process). The stability of the mixtures is also very high. Surface relief diffraction gratings were inscribed on these systems. The measured diffraction efficiency was about 0.25% for a diamine-doped polyimide exposed for 1 h to an irradiance of 200 mW/cm^2. The surface profile studied by atomic force microscopy showed an amplitude of 30 nm and a regular spacing of 700 nm on a 255 nm thick film. The photoinduced gratings had a high stability without further surface deformation after baking at 240 °C for 1 h in air.

Introduction

Azo-dye-containing organic and polymeric materials are promising materials for optical applications. They have been the subject of intensive research during the past few years for photofunctional applications in nonlinear optics (NLO),[1] in optical memory,[2] and as photoswitching devices,[3] and their potential as photorefractive materials has also been demonstrated.[4]

The amorphous azo-containing polymers can exhibit reversible birefringence and linear dichroism,[5−8] and stable holographic surface relief gratings have also been recorded on such amorphous thin films.[9−14] The photoinduced birefringence is a consequence of the reversible trans ↔ cis photoisomerization with respect to the N═N double bond of the azobenzene group, which induces an angular redistribution in the orientation of the photochromic entities. Because of the selectivity of excitation, the chromophores will tend to orient in a direction perpendicular with respect to the polarization of the actinic light. After the laser pump is turned off, the photoinduced orientation is relatively stable depending on the polymer matrix properties such as glass transition temperature, molecular weight, polarity, position of the azo group, etc. The chromophore can be either dispersed in the polymer matrix or bound in the main chain or side chains. In all cases, the structural and dipolar properties of the azo unit and its content in the sample are factors that play an important role during the orientation processes. Side-chain polymers are more attractive than doped systems because typically more than 80% of the birefringence can still be observed after a long relaxation period. This remnant birefringence can be erased by heating the polymer film above its T_g or, locally, by using circularly polarized light to restore an isotropic distribution.

The stability and the magnitude of induced birefringence and surface gratings are strongly associated with polymer properties such as the chromophore structure, the polymer main chain rigidity, and the interaction between the chromophore and the main chain. In an effort to increase the stability of the optically induced birefringence for long-term optical storage applications, new azopolymers are being designed and synthesized. Polyimides have been extensively studied because of their high thermal stability characterized by high glass transition temperature (T_g) and high thermal decomposition temperature (T_d).[15] In light of these properties, fully functionalized azo-containing polyimides have been synthesized, and their optical properties such as NLO and photorefractivity have showed great thermal stability.[16−21] In terms of thermal stability, it is well-known that an all-aromatic azo chromophore (Chart 1a) has a higher stability than an alkyl-linked azo chromophore (Chart 1b).[22] On the basis of such an assumption, we have designed a new aromatic azo chromophore whose structural unit is shown in Chart 1c. The azo chromophore is directly linked with a carbazole chromophore, and the overall structure is asymmetric. Such an all-aromatic chromophore embedded into polyimides is expected to produce high thermal stability, which, in turn, could stabilize optical properties. The photoconductive carbazole moiety can afford possible photorefractive properties.[6]

We present here the details of monomer and polyimide syntheses and of the optical studies including optically induced birefringence and holographic surface grating inscription. Photorefractive properties will be investigated in a subsequent report.

Several polyimide samples were doped with Disperse Red 1 (Chart 1b; DR1-m-polyimide) or with an azocarbazole diamine (compound **4**, Scheme 1; **4**-m-polyimide). Their films, and a film of poly(methyl methacrylate) (PMMA) doped with compound **4** (**4**-m-PMMA), were also subjected to optical studies for comparison.

Experimental Section

Materials. Carbazole, copper(II) nitrate hemipentahydrate ($Cu(NO_3)_2 \cdot 2.5H_2O$), 1-fluoro-4-nitrobenzene, cesium fluoride

† Queen's University.
‡ Royal Military College.
* Corresponding author.

10.1021/ma990753+ CCC: $18.00
Published on Web 11/13/1999

Chart 1

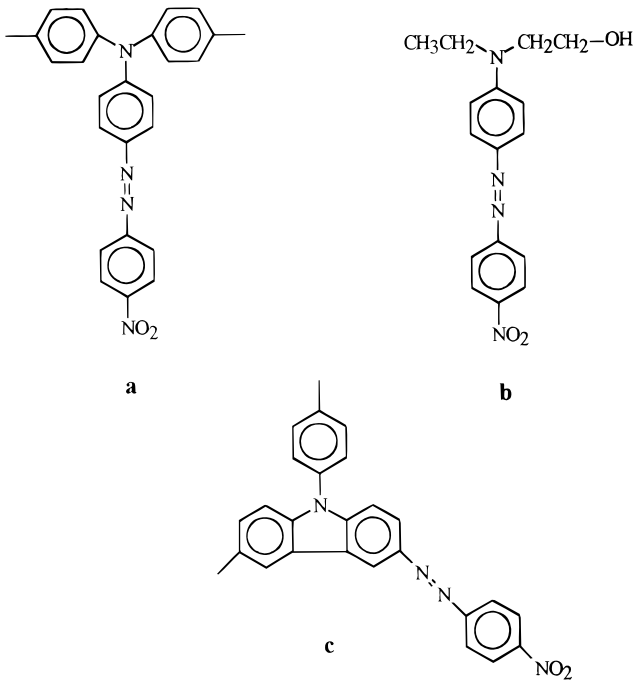

(CsF), granulated tin, acetic acid, and acetic anhydride were purchased from Aldrich Chemical Co. and used as received. 4,4′-(Hexafluoroisopropylidene)diphthalic anhydride (6FDA) (99%, Aldrich Chemical Co.) was recrystallized from acetic anhydride and dried at 100 °C under high vacuum for 48 h. 1-Methyl-2-pyrrolidinone (NMP) was vacuum-distilled from calcium hydride.

Chemical Characterization. ^{1}H, ^{13}C, and 2D-COSY NMR spectra were recorded on a Bruker AC-F200 NMR spectrometer or on a Bruker AM400 NMR spectrometer in $CDCl_3$, acetone-d_6, or DMSO-d_6. UV−vis spectra were recorded on a Hewlett-Packard UV−vis spectrometer in THF at room temperature. Gel permeation chromatography (GPC) analysis was performed on a Waters Associates model 400 liquid chromatograph equipped with a UV (254 nm) detector using THF as an eluent at a rate of 1.0 mL/min and polystyrenes as standards. Thermal analysis was performed on a Mettler differential scanning calorimeter (DSC) with a TA3000 thermal analysis system equipped with a TC10A TA processor and a DSC30 head. Mass spectra were obtained from a VG Quattro mass spectrometer. IR spectra (KBr pellets) were recorded on a Bomem MB-120 FTIR spectrophotometer.

Monomer Synthesis. 3,6-Dinitrocarbazole (1). $Cu(NO_3)_2 \cdot 2.5H_2O$ (14 g, 60 mmol) was added into a mixture of acetic acid (25 mL) and acetic anhydride (50 mL) at room temperature. The mixture was stirred for 10 min, and to this solution was then added carbazole (8.35 g, 50 mmol) in portions. Heat was generated during the addition, and 25 mL of acetic acid was added afterward. The mixture was stirred for 15 min and then poured into distilled water (500 mL). The precipitate was collected by filtration and washed with water (300 mL × 3). The still wet product was then dissolved into a potassium alcoholic aqueous solution (KOH, 50 g; water, 500 mL; and ethanol, 500 mL). The solution quickly became red. After being stirred for 30 min, the solution was filtrated, and the filtrate was acidified with concentrated hydrochloric acid. The yellow precipitate was then collected by filtration, washed with water until neutral, and then dried at 100 °C under vacuum. Yield was 11.0 g (85%); mp 240 °C (DSC in air). IR (KBr): 3395, 3082, 1634, 1612, 1579, 1517, 1307, 1102, 752, 718 cm^{-1}. ^{1}H NMR (200 MHz, acetone-d_6): δ 9.34 (d, 2H, J = 2.3 Hz), 8.40 (dd, 2H, J = 2.3 Hz, J = 8.9 Hz), 7.78 (d, 2H, J = 8.9 Hz). MS (EI, *m/e*, % relative intensity): 257 (M^+, 100).

3,6-Dinitro-*N*-(4′-nitrophenyl)carbazole (2). To a round-bottom flask were added 3,6-dinitrocarbazole (5.30 g, 20.6 mmol), 1-fluoro-4-nitrobenzene (2.95 g, 20.9 mmol), CsF (4.73 g, 30.9 mmol), and dry DMSO (80 mL). The mixture was refluxed under argon for 24 h. The solution was then cooled and poured into a mixture of water (500 mL) and methanol (500 mL). The precipitate was collected by filtration, washed with water, alcoholic potassium hydroxide, and methanol, and dried at 150 °C under vacuum. Yield was 6.30 g (82%); mp 262 °C (decomposition, DSC in air). IR (KBr): 3082, 1590, 1508, 1320, 1169, 850, 753 cm^{-1}. MS (EI, *m/e*, % relative intensity): 378 (M^+, 30). No NMR data were obtained due to insolubility in deuterated organic solvents.

3,6-Diamino-*N*-(4′-aminophenyl)carbazole (3). Compound **2** (4.00 g, 10.60 mmol) and granulated tin (6 g, 50 mol), along with concentrated hydrochloric acid (100 mL), were placed into a round-bottom flask. The mixture was refluxed under argon for 24 h. The solution was then cooled to room temperature and poured into an aqueous sodium hydroxide solution (20%, 500 mL). The precipitate was collected by filtration and washed with water. The product was extracted with THF, and the THF solution was dried over $MgSO_4$ and filtrated. The THF solution was concentrated and poured into stirred hexane (400 mL). The precipitate was collected by filtration and dried at 70 °C under vacuum overnight. Yield of the solid product: 2.30 g (75%); mp 220 °C (decomposition, DSC in air). IR (KBr): 3229, 3212, 1658, 1590, 1500, 1448, 1363, 1212, 830, 750, 699 cm^{-1}. ^{1}H NMR (200 MHz, DMSO-d_6): δ 7.0−7.2 (m, 4H), 6.93 (d, 2H), 6.6−6.8 (m, 4H), 4.86 (s, br, 6H, $3NH_2$). ^{13}C NMR (50.3 MHz, DMSO-d_6): δ 139.41, 129.64, 126.65, 126.49, 119.03, 115.71, 110.71, 110.51, 109.92, 105.84. MS (EI, *m/e*, % relative intensity): 288 (M^+, 100). This compound was used without further purification for the next reaction.

Azocarbazole Diamine (4). Compound **3** (2.88 g, 10 mmol) was dissolved into a mixture of THF (10 mL) and acetic acid (10 mL). To this was added 4-nitronitrosobenzene[23] (1.52 g, 10 mmol) dissolved in THF (10 mL) for 10 min. After being stirred at room temperature under argon for 6 h, the mixture was poured into a 200 mL ice-cooled 20% potassium carbonate solution containing 200 mL of ethyl acetate. The mixture was filtered through a Celite, and the layers were separated. The aqueous layer was extracted with an additional 150 mL of ethyl acetate. The combined ethyl acetate solution was washed with water and dried over $MgSO_4$. After evaporation, the residue was purified through silica gel column eluting with ethyl acetate−hexane (gradient elution, 30−60% ethyl acetate). Recrystallization from toluene gave brown product in 0.85 g (20% yield); mp 240 °C (decomposition, DSC in air). IR (KBr): 3362, 1170, 1597, 1517, 1335, 1297, 1102, 855 cm^{-1}. ^{1}H NMR (400 MHz, DMSO-d_6, see Scheme 1 for labeling): δ 9.18 (s, 1H, H_4), 8.42 (s, 1H, H_5), 8.38 (d, 2H, $H_{2'',6''}$, J = 9.2 Hz), 7.92 (d, 2H, $H_{3'',5''}$, J = 9.20 Hz), 7.30 (d, 1H, H_2, J = 9.2 Hz), 7.23 (d, 1H, H_8, J = 8.4 Hz), 7.0−7.2 (m, 4H, $H_{1,8,2'6'}$), 6.80 (d, 2H, $H_{3',5'}$, J = 8.8 Hz), 5.50 (s, br, 4H, $2NH_2$ on the carbazole ring), 4.93 (s, br, 2H, NH_2 on the 9-phenyl ring). ^{13}C NMR (50.3 MHz, DMSO-d_6): δ 139.41, 129.64, 126.65, 126.49, 119.03, 115.71, 110.71, 110.51, 109.92, 105.84. UV−vis (THF, λ_{max}): 306, 372, and 494 nm (broad). MS (EI, *m/e*, % relative intensity): 422 (M^+, 20).

Azocarbazole Polyimide. Diamine **4** (146 mg, 0.345 mmol) was dissolved into 1.5 mL of NMP. To this was added 6FDA (153 mg, 0.345 mmol) and an additional 1.5 mL of NMP. The polymerization solution was stirred at room temperature under argon for 48 h, yielding a viscous polyamic acid solution. To the above solution were added 2 mL of acetic anhydride and 1 mL of pyridine. The solution was stirred for an additional 12 h at room temperature and 6 h at 90 °C. The mixture was then poured into methanol (200 mL). The precipitate was collected by filtration. The polymer was redissolved into a small amount of THF (10 mL) and reprecipitated from methanol (500 mL). The precipitate was filtrated and dried at 70 °C under high vacuum overnight. IR (KBr): 1786, 1725, 1601, 1517, 1342, 721 cm^{-1}. ^{1}H NMR (200 MHz, DMSO-d_6): see Figure 2. UV−vis (polymer film, λ_{max}): 234, 284, 372 nm (broad).

Scheme 1. Synthesis of Monomer 4

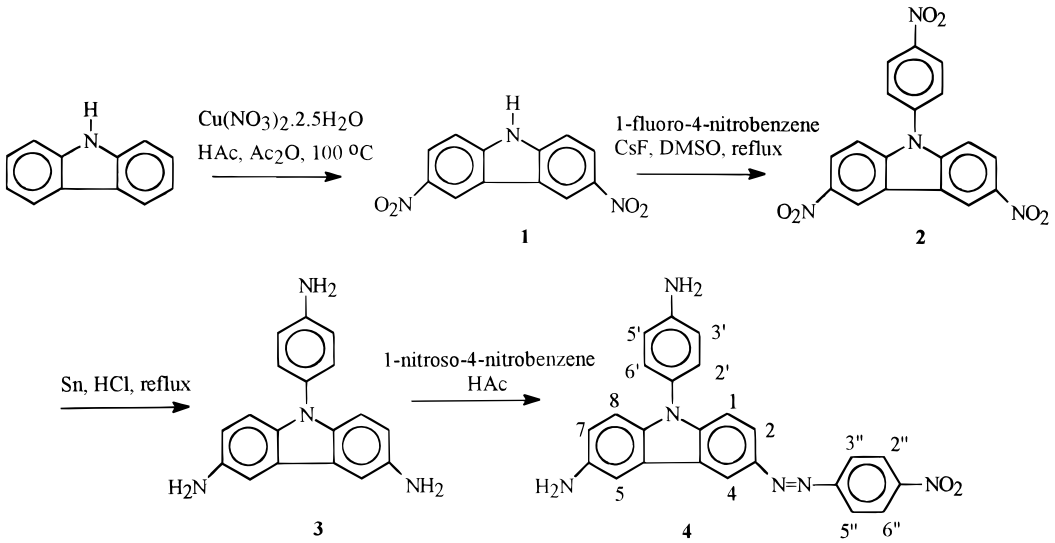

Anal. Calcd for $C_{24}H_{18}N_6O_2$: C, 68.24; H, 4.29; N, 19.89. Found: C; 68.05; H, 4.30; N, 19.63.

Polymer Films and Optical Studies. Thin films of azocarbazole polyimide were obtained by dissolving this polyimide in dry THF (5 wt %). The solutions were filtered and deposited by spin-coating onto glass substrate.

Polyimide samples doped with Disperse Red 1 (DR1-m-polyimide) or with compound **4** (**4**-m-polyimide) were prepared with 1:1 molar ratio of dopant to the structural unit. To evaluate the properties of compound **4** alone, a solution of monodisperse PMMA (M_w = 120 000) containing 10% w/w of compound **4** has also been prepared using chloroform as solvent. The films were allowed to dry and subsequently heated at 70 °C in an oven for 24 h. Homogeneous thin films with a thickness from 250 to 300 nm (for the polyimide films) and about 1000 nm for **4**-m-PMMA were obtained. The procedure for measuring the optically induced and erased birefringence can be found elsewhere.[8] In typical experiments, the photoorientation period (1500 s), using linearly polarized light, is followed by a relaxation period without illumination of the same length and by an erasing period of 500 s when circularly polarized light is used. These experiments were performed at room temperature using an argon laser (λ_{pump} = 488 nm) with an irradiance of 100 mW/cm^2. The birefringence was detected using a weak diode laser beam at 674 nm as a probe. The time resolution of the experimental data during photoinduced orientation and during relaxation is 1 point/s. Surface profile gratings were inscribed using the co- and contracircularly interfering beams. Details about optical setup have been previously described.[9,13] The dynamic diffraction efficiencies of the positive first order were measured on 700 nm spacing grating with a time resolution of 1 point/s. The surface relief characteristics have then been checked using an atomic force microscope.

Results and Discussion

Materials. Monomer Synthesis. In general, an azobenzene chromophore can be obtained by a coupling reaction between an electron-poor diazonium salt and an electron-rich aromatic compound with fairly good solubility in water.[23] The coupling reaction occurrs in an aqueous medium. This works well for the preparation of many azo aromatic compounds. It is also found that azocarbazole compounds can be synthesized by using such coupling reaction with the aid of a phase transfer catalyst in a two-phase medium.[24] Post-azo-coupling reactions have also been successful in some polymer systems where the electron-rich aromatic position on the polymer side chain is capable of coupling with a diazonium salt in an organic solvent.[25] However, the synthesis of the desired diaminocarbazole monomer **4** could not be performed by diazonium coupling.[26] It has been reported that a coupling reaction between an aromatic amine and a nitroso compound catalyzed by acetic acid provides an alternative way to synthesize azobenzene derivatives.[16] Scheme 1 shows the synthesis of this monomer employing this methodology.

Carbazole was first dinitrated with $Cu(NO_3)_2 \cdot 2.5H_2O$ in the mixture of acetic acid and acetic anhydride at around 100 °C. The resulting dinitrocarbazole **1**, when reacted with 1-iodo-4-nitrobenzene using the classical Ullmann condensation,[27] did not give the desired trinitro compound **2**. However, when it was reacted with 1-fluoro-4-nitrobenzene catalyzed with CsF, trinitrophenylcarbazole **2** was easily obtained in high yield. It is believed that CsF acts as both activation agent of the free 9-amino group on carbazole **1** and an acceptor of the HF or as a base.[28] Reduction of trinitrophenylcarbazole **2** with granulated tin in hydrochloric acid under reflux gave the triaminophenylcarbazole **3**. Subsequent nitroso coupling reaction of this compound with 1-nitro-4-nitrosobenzene in a 1:1 molar ratio gave monomer **4**. Interestingly, no symmetric product was obtained, due to the different reactivities of the two types of amino groups on compound **3**, one type on the 9-phenyl ring and the other type on the carbazole ring. The latter have higher electron density due to the strong carbazole electron-donating nature, thus having higher reactivity with the nitroso group and eventually form the asymmetric azodiamino compound **4**. The structure of this monomer has been confirmed by NMR, MS, and IR. The melting point of this monomer is 240 °C (decomposition) as obtained by DSC.

Polyimide Synthesis and Characterization. Polymerization of the monomer **4** and 6FDA in the 1:1 molar ratio in NMP at room temperature gave polyamic acid, and the addition of a mixture of acetic anhydride and pyridine gave the polyimide in quantitative yield (Scheme 2).

Dianhydride 6FDA was used to ensure that the resulting polyimide has good solubility and film formability.[29] The weight-average molecular weight of this polyimide as determined by GPC is 1.6×10^4, relative to polystyrene standards, and the polydispersity index

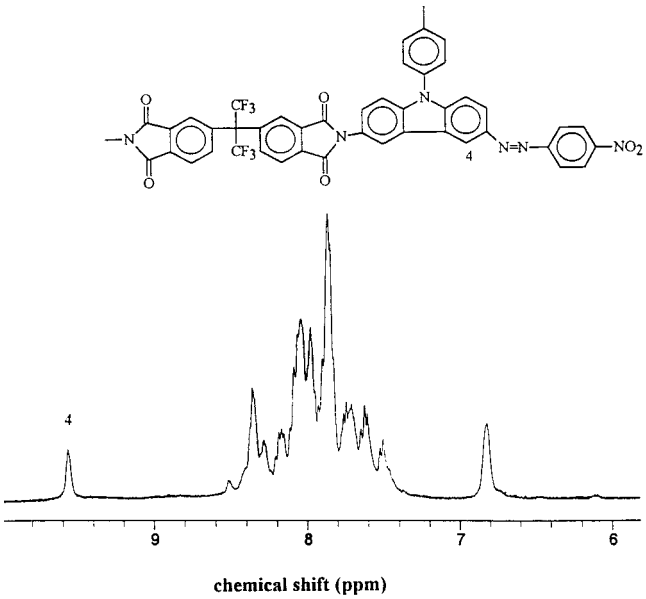

Figure 1. ^{1}H NMR spectrum (400 MHz, DMSO-d_6) of the azocarbazole polyimide.

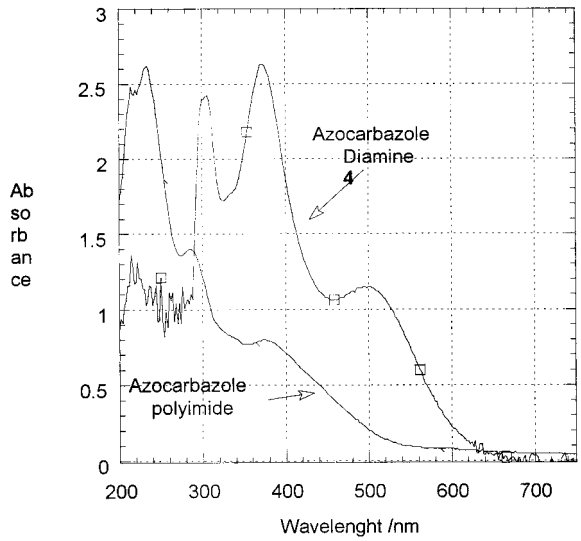

Figure 2. UV−vis spectra of compound **4** in THF and of the azocarbazole polyimide film at room temperature.

is 1.9. This polyimide is quite soluble in many polar organic solvents such as NMP, DMF, DMSO, and THF. The asymmetric structure of the polymer repeating unit is probably responsible for its solubility in these solvents. The IR spectrum shows characteristic imide peaks at 1786 and 1725 cm^{-1} and nitro peaks at 1517 and 1342 cm^{-1}. Figure 1 shows the ^{1}H NMR spectrum of this polyimide. A singlet at 9.51 ppm is assigned to the proton at the 4-position in the carbazole ring, due to the strong electron-withdrawing character of the azo chromophore.

The UV−vis spectra of monomer **4** in THF and of the polyimide film at room temperature are shown in Figure 2. Monomer **4** shows two absorption maxima at 306 and 372 nm, characteristic of the carbazole chromophore, and a broad peak at 494 nm due to the $\pi-\pi^*$ transition of the azocarbazole chromophore. In comparison, the azocarbazole polyimide shows absorption maxima at 234 nm due to the aromatic rings, at 284 nm characteristic of the carbazole chromophore, and at 372 nm due to the $\pi-\pi^*$ transition of the azocarbazole chromophore. An important blue shift (122 nm) is observed between the monomer and the polyimide. This happens because the dipole moment is significantly different in the two cases. The monomer has a relatively high dipole moment due to the high charge-transfer between the electron-donor groups of the 6-aminocarbazole ring and 9-(4′-amino)-phenyl ring and the nitro acceptor group. In the polyimide, the imide groups bound to the carbazole and 9-phenyl rings are weak electron acceptors, thus decreasing the overall dipole moment in the azocarbazole chromophore.

Scheme 2. Synthesis of Azocarbazole Polyimide

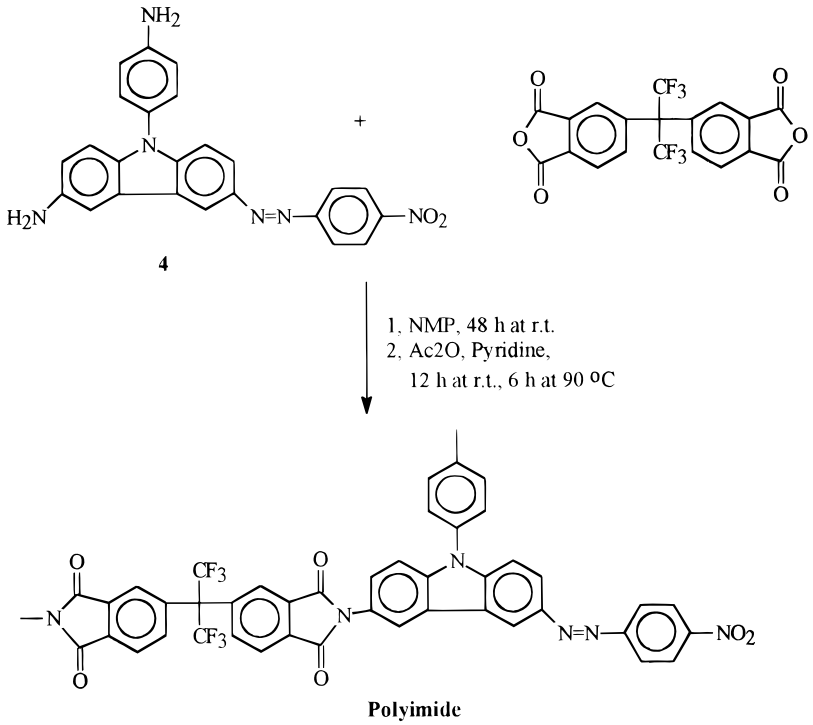

Table 1. Parameters Obtained by Fitting the Orientations Curves of Birefringence Data with Eq 1

sample	A	k_w (s^{-1})	β_w	$\langle k_w \rangle$ (s^{-1})
polyimide	0.0360 ± 0.0001	0.0064 ± 0.0001	0.4529 ± 0.0011	0.00265
4-m-polyimide (1:1 molar)	0.0704 ± 0.0001	0.0121 ± 0.0001	0.5495 ± 0.0001	0.00709
DR1-m-polyimide (1:1 molar)	0.0639 ± 0.0001	0.0290 ± 0.0001	0.3693 ± 0.0019	0.00690
4-m-PMMA (10% w/w)	0.0062 ± 0.0001	0.0010 ± 0.0001	0.5094 ± 0.0009	0.00052

Table 2. Parameters Obtained by Fitting the Relaxations Curves of Birefringence Data with Eq 2

sample	B	C	k_r (s^{-1})	β_r	$\langle k_r \rangle$ (s^{-1})	$-\Delta n_{max}$	Cn (%)
polyimide	0.0289 ± 0.0003	0.0048 ± 0.0003	(5.2 ± 1.4) × 10^{-5}	0.2990 ± 0.0056	5.6 × 10^{-6}	0.0339	86
DR1-m-polyimide (1:1 molar)	0.0511 ± 0.0001	0.0111 ± 0.0001	0.0359 ± 0.0004	0.3238 ± 0.0015	0.00534	0.0622	82
4-m-polyimide (1:1 molar)	0.0689 ± 0.0001	0.0019 ± 0.0001	0.0073 ± 0.0003	0.4577 ± 0.0131	0.00306	0.0707	97
4-m-PMMA (10% w/w)	0.0025 ± 0.0001	0.0019 ± 0.0001	0.0014 ± 0.0001	0.4849 ± 0.0003	0.000655	0.0044	56

[a] Cn = $C/(C + B)$.

The thermal properties of this polyimide were analyzed by DSC in air. No glass transition temperature was observed, due to the rigid backbone. The onset decomposition temperature was 370 °C.

Optically Induced and Erased Birefringence. To analyze the phenomena occurring during the angular redistribution of the azo moieties in the polyimide films, in-situ birefringence measurements were performed during writing cycles (linearly polarized pump on), relaxation cycles (pump off), and photoinduced erasing processes (circularly polarized pump on).

A quantitative analysis of orientation and relaxation curves of Δn (birefringence) is presented, using the Kohlraush−Williams−Watts (KWW) function, the so-called stretched exponential. Relevant parameters extracted from the fit are discussed for both orientation and relaxation processes for the various thin films (Tables 1 and 2).

It appears that at least two regimes are involved during the photoinduced orientation process. The fast one is due to the pump condition and quantum yield of photoisomerization according to the angular hole burning model introduced by Dumont et al.[30] The mechanism of photoinduced birefringence is based on the selective photochemical excitation of trans chromophore having a component of their dipole in the same direction as the laser polarization. The trans chromophore will undergo trans−cis−trans photoisomerization cycles, accompanied by a change of orientation of the chromophores toward the perpendicular direction with respect to the polarized light. This uniaxial angular reorientation induces a strong modification of the optical properties by increasing the chromophore population in the perpendicular direction, creating birefringence and linear dichroism.

However, the dynamics of these photophysics processes (photoisomerization and angular reorientation) are strongly dependent on various factors, such as the size and the polarity of the photochromic group, the nature and the tacticity of the polymer matrix, and the T_g of the polymeric material. Previous studies have shown that the kinetics of the thermal cis-to-trans back-relaxation of an azo chromophore embedded in a polymer matrix is very sensitive to the structure, morphology, and viscoelastic properties of the polymer.[5]

In addition, cooperative motions between photoactive and nonphotoactive group in functionalized polymers indicate that dipolar interactions are more important than steric ones.[31,32] Furthermore, from molecular dynamics experiments made using polarization modulation in infrared spectroscopy, it has been demonstrated that the slow and fast processes are not directly associated with main-chain segment motions.

Using these polyimide materials, it can be expected that the photoisomerization efficiency and the reorientation motions of the side-chain chromophores will be strongly constrained by the polyimide matrix due to several factors such as the T_g, rigidity of the carbazole backbone, and weak resonance conditions during the irradiation process.

Quantitative Analysis of the Orientation and Relaxation Processes. The time dependence of the birefringence during orientation and relaxation period can be described quite well by a biexponential function. From these results, a fast and a slow regime can be separated, and an estimate of the dominant processes can be made considering the respective weight of each process. The extracted exponential constants may be associated with the lifetime of the cis isomer for the fast process, while the dipole reorientation involving motions of the polymer may be associated with the slow process.[33]

This approach is not very useful for the analysis of very constrained polymers since it is difficult to unambiguously separate a fast and a slow process. To consider a distribution of photoactive entities in various surroundings, a stretched exponential can also be used to describe the dynamic behavior in azo polymers thin films. Thus, the orientation and relaxation curves of the polyimide-based films were fitted using a stretched exponential.[32,34]

The orientation curve of the birefringence can be described by the function

$$\Delta n = A(1 - \exp(-k_w t)^{\beta_w}) \quad (1)$$

where A is the maximum birefringence, k_w is the rate constant of the birefringence growth, and β_w is the width of the rate constant distribution.

Similarly, the relaxation curves were fitted by the function

$$\Delta n = B + C \exp(-k_r t)^{\beta_r} \quad (2)$$

where B is the extrapolated birefringence after long relaxation time, and the quantity $B + C$ is the maximum induced birefringence just before turning the pump off; k_r is the rate constant of the birefringence relaxation, and β_r represents the width of the distribution. If $\beta =$

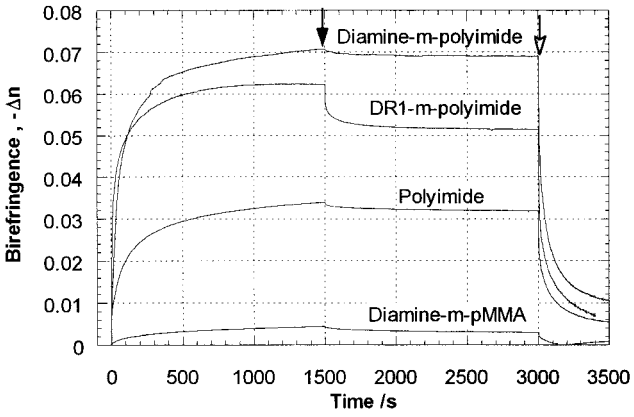

Figure 3. Optically induced birefringence in the polyimide film using an argon laser (488 nm). The linearly laser pump is turned on at $t = 0$ for 1500 s. The laser is turned off at $t =$ 1500 for a 1500 s relaxation period (black arrow). An erasing circularly polarized beam is turned on at $t = 3000$ for 500 s (white arrow).

1, the dynamics display a monoexponential growth or decay, and only one kind of interaction is present; $\beta \neq 1$ indicates a wide distribution of the time constants due to the inhomogeneity of the various constraints.

To compare the orientation and relaxation dynamics in various samples, an average rate constant $\langle k \rangle$ can be defined considering the rate constant k_w or k_r and the width of the distribution.

$$\frac{1}{\langle k \rangle} = \int_0^\infty \exp[-(kt)^\beta]\, dt = \frac{\Gamma(1/\beta)}{k\beta} \qquad (3)$$

(a) Orientation Behavior. The best fit parameters calculated for Δn measurements over a 1500 s time range for the various systems are reported in Table 1. The polyimide displays a slow increase of the birefringence, and even after 1500 s of irradiation at 100 mW/cm^2 the plateau value is not reached (Figure 3). Experiments over a longer time range have been performed, and even after 3500 s no plateau value is reached. The maximum birefringence is about 0.035, which can be compared with previously published doped systems such as DR1-m-PMMA.[32] Since the dipole moment of the polyimide chromophore is smaller than that of DR1-like chromophores in other azo-containing polymer systems, because of the electron-withdrawing nature of imide groups, the weak absorbance at 488 nm produces slower and weaker photoisomerization and reorientation motions, so that the photoinduced birefringence is less efficient. The width of the distribution is $\beta = 0.453$, meaning that a large distribution of the constraints is governing the reorientation processes. This value is far from those obtained for poly{[4′-[[2-(methacryloyloxy)-ethyl]ethylamino]-4-nitroazobenzene} (pDR1M) or poly-[4-(2-methacryloyloxy)ethyl-azobenzene] (pMEA) polymers, where the distribution width is about 0.8.[34]

The **4**-m-polyimide film displays a narrower distribution factor ($\beta_w = 0.549$). This observation proves the dipolar and steric compatibility of the azocarbazole polyimide and the azocarbazole diamine. In the case of DR1-m-polyimide the width of the distribution indicates a wide variety of constraints probably due to the differences of morphologies between a rodlike molecule (DR1) and an azocarbazole derivative ($\beta = 0.369$). Moreover, it appears that the DR1 molecules isomerize and reorientate faster in the polyimide matrix because the free volume may be larger than in a conventional polymer matrix such as PMMA.

The extracted average rate constants for **4**-m-polyimide, $\langle k_w \rangle = 0.00709$, and for DR1-m-polyimide, $\langle k_w \rangle = 0.0069$, are more than twice that observed for the pure polyimide, $\langle k_w \rangle = 0.00265$. The explanation of this difference is probably the change in the glass transition temperature when doping small molecules in the rigid polyimide. Since all materials decomposed before going through their glass transition, it was not possible to measure the T_g's, but it can be assumed that the T_g is significantly depressed by the addition of either DR1 or **4**. The decomposition temperatures of the doped polyimide materials are indeed lower (150 °C for the DR1-doped and 240 °C for the **4**-doped, as compared with 370 °C for the pure polyimide). One can assume that the mobility of the azo chromophore, either bound or dissolved in the material, is much higher when the glass transition temperature of the material is lower.

Surprisingly, the induced birefringence in **4**-m-PMMA is quite weak and slow to build up, which is certainly due to the relatively high molecular weight of the PMMA (M_w= 120 000 g/mol) which causes steric hindrances in the reorientational motion of the larger azocarbazole diamine moieties. In addition, the distribution width ($\beta = 0.5094$) is narrower than in DR1-m-PMMA thin films, typically around $\beta = 0.3$.[32] This may happen because of the bulkiness of **4** as compared to DR1. The highest birefringence ($\Delta n = 0.07$) is reached for resonant systems where the absorption band of the thin film is near the resonant conditions. The **4**-m-polyimide has an absorbance of about 1 at 488 nm, which is enough to improve the performance of the photoinduced orientation process.

(b) Relaxation Behavior. The main feature of the polyimide materials is the stability of the optically induced birefringence. In the case of the polyimide and the **4**-m-polyimide, the remnant birefringence is very stable at about 86% for the pure polyimide and, surprisingly, 97% for the doped polyimide. Moreover, the induced birefringence is quite stable even after relatively harsh thermal treatment (1 h at 240 °C).

The DR1-m-polyimide has a remnant birefringence of 82%, which means that the free volume is large enough for some DR1 molecules to reorient. In the case of **4**-m-polyimide, the diamine molecules are more constrained.

The analysis of time constants reveals that the relaxation processes are slower for the polyimide ($\langle k_r \rangle = 5.6 \times 10^{-6}$) and **4**-m-PMMA ($\langle k_r \rangle = 6.5 \times 10^{-4}$) while the blended polyimide such as **4**-m-polyimide ($\langle k_r \rangle =$ 0.00306) and DR1-m-polyimide ($\langle k_r \rangle = 0.00534$) have faster and similar relaxation constants. Such relatively slow relaxation processes can be explained on the basis of nature of the chromophore and polymer structure. In the pure polyimide, the chromophore has a fairly restricted reorientational motion, since the azo group is covalently bound to the carbazole unit, while in other azo-containing polymethacrylate-like polymers, the azo chromophores are bridged with a flexible alkyl group to the main chain and are allowed more free motion. These properties may be also responsible for the low degree of orientation and for the low efficiency of the thermal relaxation.

The same observation made for **4**-m-PMMA is in agreement with the previous comments for the orientation process, i.e., confirming the steric incompatibility

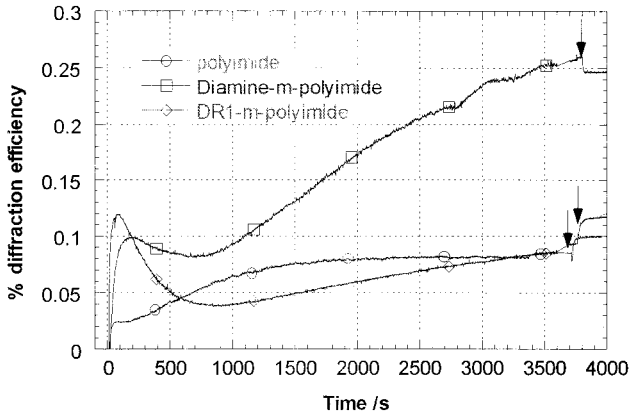

Figure 4. Diffraction efficiency of surface gratings inscribed on the azocarbazole polyimide thin film (255 nm) as a function of irradiation time. The argon ion beam is at 488 nm with an irradiance of 200 mW/cm^2. The pump is turned off after approximately 3700 s (black arrows).

of the relatively large dispersed diamine monomer strongly constrained in small PMMA free volumes. For both DR1-m-polyimide and **4**-m-polyimide, the faster rate constants indicate that the dispersed chromophores in the amorphous polymer have more freedom to move in the bulk.

An interesting result is that the distribution width parameter, β, has the same magnitude for polyimide and for DR1-m-polyimide, revealing a large range of constraints in the bulk during the relaxation process ($\bar{\beta} \cong 0.3$). The distribution is narrower when larger molecules, such as **4**, are dissolved into the polyimide. It is reasonable to assume some kind of interaction between the doped diamine and the bound chromophore of the polyimide. The narrower distribution for **4**-m-polyimide may be due to a preferred ordering of the two types of azo chromophores in the material. In addition, as previously discussed, the steric factor must also be considered; thus, more uniformity in the type of constraints could be expected when the inserted molecule is larger, leading to a larger β value.

Laser-Induced Surface Inscription. Surface relief gratings have been inscribed on both the pure polyimide and the doped polyimide films, using left and right circularly polarized interfering beams ($\lambda_{pump} = 488$ nm, 200 mW/cm^2). In Figure 4, the time-dependent diffraction efficiency recorded on the first diffraction order using a linearly polarized probe is shown. The grating inscription process can be divided into three stages according to the slope of the diffraction efficiency versus exposure time. As shown in Figure 4, the three experimental curves exhibit an initial an rapid growth (on the order of tens of seconds) of the diffraction efficiency up to $\eta = 0.1\%$ for the doped polyimides and less than 0.03% for the pure polyimide, corresponding to the formation of the reversible volume birefringence gratings. As confirmation, AFM measurements show no surface grating for this first period.

In the second stage, the diffraction efficiency decreases for the doped polyimides and stays relatively constant for the polyimide. At this time, the formation of surface relief grating starts and strongly interferes with the phase (birefringence) grating. After this, a monotonic increase of the diffraction efficiency is observed over a 1 h inscription period. A plateau value is reached for the polyimide after about 1500 s, while the doped polyimide films still show an increase in the

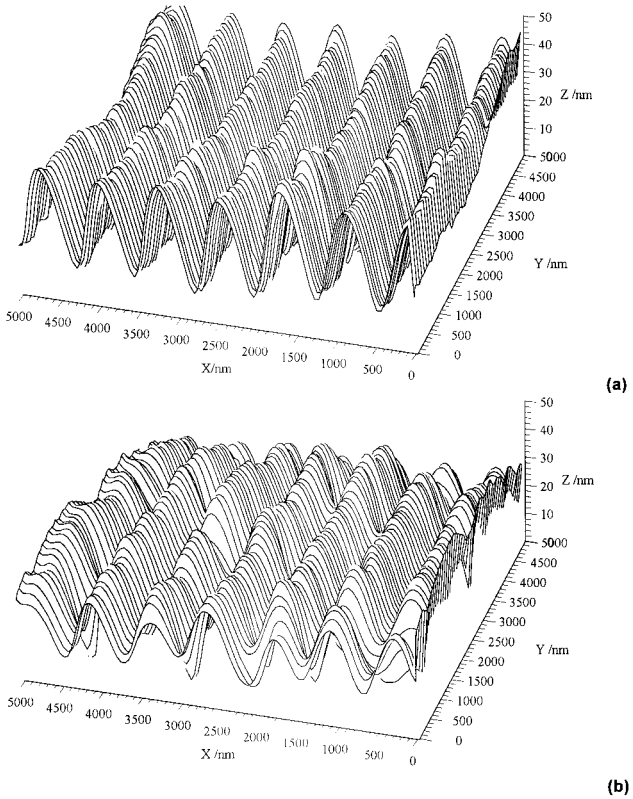

Figure 5. AFM surface grating profile of the azocarbazole polyimide (b) and **4**-m-polyimide (a) thin films. The same profiles are observable after heating 1 h at 240 °C.

grating diffraction efficiency. It is important to note that all the films have the same thickness (250 ± 10 nm). Therefore, it is apparent that the inscribed diffraction gratings have a low diffraction efficiency (the highest is $\eta = 0.25\%$ for **4**-m-polyimide) as compared with those of other azo polymers studied in our group.[13,14] This is probably due to the restricted motions in the polyimide. Although the low extinction coefficient of this polyimide at the writing wavelength (488 nm) is probably not a significant factor,[10] the low mobility of the whole polymer chain due to its rigidity may be a major one.

After the writing beam is turned off, a fast relaxation of the diffraction efficiency occurs. This observation suggests the formation of both a phase grating (refractive index modulation) and a surface relief grating, in agreement with previous real-time measurements of diffracted orders during the grating formation.[35] If the surface relief is the dominant effect, a significant increase in efficiency is seen when the pump is turned off, while if the phase grating is dominant, the efficiency decreases. The first observation is still puzzling, but it has been suggested that it could be due to the thermal and mechanical stabilization of the polymer mass transport when the pump is turned off. The decrease in efficiency for phase gratings is easily explained by the angular relaxation process of the chromophores.

AFM scans of the surface relief gratings are shown in Figure 5. For the pure polyimide, the maximum amplitudes of the surface relief do not exceed 20 nm while amplitudes greater than 35 nm were obtained for the **4**-m-polyimide. The grating modulation profile on the film surface exhibits a regularly spaced and sinusoidal shape with grating spacings of 700 nm. Since the polyimide does not exhibit glass transition prior to thermal decomposition at 370 °C (240 °C for **4**-m-

polyimide), thermal erasing of this grating for reversible optical storage is not possible. After annealing the inscribed gratings on the polyimide film for 1 h at 240 °C in air, no surface relief deformation or depth changes were observed, confirming the high stability of the surface modification.

Conclusions

A new azocarbazole diamine monomer (compound **4**) was synthesized, and the soluble polyimide derived from this monomer showed high thermal stability ($T_d = 370$ °C in air). Optical properties of this polyimide were studied. Reversible optically induced birefringence on polyimide films was obtained. A very high stability of the birefringence was observed after turning off the linearly polarized laser light. Because of the weak absorption coefficient of the pure polyimide at 488 nm, doped systems with compound **4** in the polyimide matrix have been analyzed. The yield of photoisomerization and reorientational processes is improved, leading to an higher maximum birefringence. This very stable birefringence can be optically erased using circularly polarized light.

Optically induced holographic surface gratings on the thin film with circularly polarized laser beams were also obtained and showed remarkable thermal stability without further surface deformation even after baking at 240 °C for 1 h in air. Experiments on the temperature dependence of photoinduced birefringence and optically inscribed surface relief gratings are under way.

Acknowledgment. Funding from the Office of Naval Research, NSERC Canada, and Department of National Defence Canada is gratefully acknowledged.

References and Notes

(1) Dumont, M.; Froc, G.; Hosotte, S. *Nonlinear Opt.* **1995**, *9*, 327.
(2) Tachibana, H.; Nakamura, T.; Matsumoto, M.; Komizu, H.; Mannda, E.; Niino, H.; Yabe, A. *J. Am. Chem. Soc.* **1989**, *111*, 3080.
(3) Xie, S.; Natansohn, A.; Rochon, P. *Chem. Mater.* **1995**, *5*, 403.
(4) Barrett, C.; Choudhury, B.; Natansohn, A.; Rochon, P. *Macromolecules* **1998**, *31*, 4845.
(5) Natansohn, A.; Rochon, P.; Meng, X.; Barrett, C.; Buffeteau, T.; Bonenfant, S.; Pézolet, M. *Macromolecules* **1998**, *31*, 1155.
(6) Ho, M. S.; Barrett, C.; Paterson, J.; Esteghamatian, M.; Natansohn, A.; Rochon, P. *Macromolecules* **1996**, *29*, 4613.
(7) Meng, X.; Natansohn, A.; Barrett, C.; Rochon, P. *Macromolecules* **1996**, *29*, 946.
(8) Natansohn, A.; Rochon, P.; Xie, S. *Macromolecules* **1992**, *25*, 5531.
(9) Rochon, P.; Batalla, E.; Natansohn, A. *Appl. Phys. Lett.* **1995**, *66*, 136.
(10) Kim, D. Y.; Tripathy, S. K.; Li, L.; Kumar, J. *Appl. Phys. Lett.* **1995**, *66*, 1166.
(11) Kumar, J.; Li, L.; Jiang, X. L.; Kim, D. Y.; Lee, T. S.; Tripathy, S. *Appl. Phys. Lett.* **1998**, *72*, 2096.
(12) Jiang, X. L.; Li, L.; Kumar, J.; Kim, D. Y.; Tripathy, S. K. *Appl. Phys. Lett.* **1998**, *72*,.
(13) Barrett, C. J.; Natansohn, A. L.; Rochon, P. L. *J. Phys. Chem.* **1996**, *100*, 8836.
(14) Barrett, C. J.; Rochon, P. L.; Natansohn, A. L. *J. Chem. Phys.* **1998**, *109*, 1505.
(15) *Polyimides;* Blackie: Glasgow, 1990; Vol; Page.
(16) Miller, R.; Burland, D.; Jurich, M.; Lee, V.; Moylan, C.; Thackara, J.; Twieg, R.; Verbiest, T.; Volksen, W. *Macromolecules* **1995**, *28*, 4970.
(17) Davey, M. H.; Lee, V. Y.; Mark, T. J.; Miller, R. D. *Polym. Prepr. (Am. Chem. Soc., Div. Polym. Chem.)* **1997**, *38*, 261.
(18) Yu, D.; Gharavi, A.; Yu, L. *J. Am. Chem. Soc.* **1995**, *117*, 11680.
(19) Saadeh, H.; Gharavi, A.; Yu, D.; Yu, L. *Macromolecules* **1997**, *30*, 5403.
(20) Yu, D.; Gharavi, A.; Yu, L. *Macromolecules* **1996**, *29*, 6139.
(21) Chen, T. A.; Jen, A. K. Y.; Cai, Y. *Macromolecules* **1996**, *29*, 535.
(22) Verbiest, T.; Burlaand, D.; Jurich, M.; Lee, V.; Miller, R.; Volksen, W. *Science* **1995**, *268*, 1604.
(23) In *Vogel's Textbook of Practical Organic Chemistry*; Furniss, B. S., et al., Eds.; 1978; Vol. 4, p 712.
(24) Ellwood, M.; Griffin, J. *J. Chem. Soc., Chem. Commun.* **1980**, 181.
(25) Wang, X.; Kumar, J.; Tripathy, S.; Li, L.; Chen, J. I.; Marturunkakul, S. *Macromolecules* **1997**, *30*, 219.
(26) Chen, J. P.; Natansohn, A.; Rochon, P., unpublished results.
(27) Gauthier, S.; Fréchet, J. *Synthesis* **1987**, 383.
(28) Imai, Y.; Ishikawa, H.; Park, K. H.; Kakimoto, M. A. *J. Polym. Sci., Part A: Polym. Chem.* **1997**, *35*, 2055.
(29) Chen, J. P.; Natansohn, A. *Macromolecules* **1999**, *32*, 3171.
(30) Sekkat, Z.; Dumont, M. *Synth. Met.* **1993**, *54*, 373.
(31) Buffeteau, T.; Natansohn, A.; Rochon, P.; Pézolet, M. *Macromolecules* **1996**, *29*, 8783.
(32) Buffeteau, T.; Lagugné Labarthet, F.; Pézolet, M.; Sourisseau, C. *Macromolecules* **1998**, *31*, 7312.
(33) Ho, M. S.; Natansohn, A.; Rochon, P. *Macromolecules* **1995**, *28*, 6124.
(34) Ho, M. S.; Natansohn, A.; Rochon, P. *Macromolecules* **1996**, *29*, 44.
(35) Lagugné Labarthet, F.; Buffeteau, T.; Sourisseau, C. *J. Phys. Chem. B* **1998**, *162*, 2654.

MA990753+